

Hard x-ray photoelectron spectroscopy study on valence band structure of semiconducting BaSi₂

Masakazu Baba, Keita Ito, Weijie Du, Tatsunori Sanai, Kazuaki Okamoto, Kaoru Toko, Shigenori Ueda, Yoji Imai, Akio Kimura, and Takashi Suemasu

Citation: *Journal of Applied Physics* **114**, 123702 (2013); doi: 10.1063/1.4823784

View online: <http://dx.doi.org/10.1063/1.4823784>

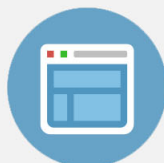
View Table of Contents: <http://scitation.aip.org/content/aip/journal/jap/114/12?ver=pdfcov>

Published by the [AIP Publishing](#)



Re-register for Table of Content Alerts

Create a profile.



Sign up today!



Hard x-ray photoelectron spectroscopy study on valence band structure of semiconducting BaSi₂

Masakazu Baba,¹ Keita Ito,¹ Weijie Du,¹ Tatsunori Sanai,¹ Kazuaki Okamoto,² Kaoru Toko,¹ Shigenori Ueda,³ Yoji Imai,⁴ Akio Kimura,² and Takashi Suemasu^{1,5}

¹*Institute of Applied Physics, University of Tsukuba, 1-1-1 Tennohdai, Tsukuba, Ibaraki 305-8573, Japan*

²*Graduate School of Science, Hiroshima University, Hiroshima 739-8526, Japan*

³*Synchrotron X-ray Station at SPring-8, National Institute for Materials Science (NIMS), Hyogo 679-5148, Japan*

⁴*National Institute of Advanced Industrial Science and Technology, AIST, Tsukuba Central 5, 1-1-1 Higashi, Tsukuba, Ibaraki 305-8565, Japan*

⁵*Japan Science and Technology Agency, CREST, Chiyoda-ku, Tokyo 102-0075, Japan*

(Received 18 May 2013; accepted 13 September 2013; published online 27 September 2013)

The valence band structures of a 35-nm-thick BaSi₂ epitaxial film on Si(111) have been explored at room temperature by hard x-ray photoelectron spectroscopy (HAXPES). The experimentally obtained photoelectron spectrum is well reproduced by first-principles calculations based on the pseudopotential method. The top of the valence band consists mainly of Si 3s and 3p states in BaSi₂, suggesting that the effective mass of holes is small in BaSi₂. This is favorable from the viewpoint of solar cell applications. The observed spectrum shifted slightly to the lower energy side due to *n*-type conductivity of BaSi₂. The valence band top was observed at about 0.8 eV below the Fermi level in the HAXPES spectrum. © 2013 AIP Publishing LLC.

[<http://dx.doi.org/10.1063/1.4823784>]

I. INTRODUCTION

It was found experimentally that semiconducting barium disilicide (BaSi₂) has a band gap of approximately 1.3 eV, matching the solar spectrum and a large absorption coefficient of $3 \times 10^4 \text{ cm}^{-1}$ at 1.5 eV.^{1,2} Migas *et al.* predicted large absorption coefficients in BaSi₂ by first-principles calculation.³ Recent experimental results on photoresponsivity, minority-carrier diffusion length and lifetime, and control of electron and hole densities by impurity doping, have spurred interest in this material for thin-film solar cell applications.^{4–9} The crystal structure of BaSi₂ has been well reported in the literature as a simple orthorhombic structure (space group *Pnma*) with a unit cell containing 8 Ba and 16 Si atoms, the latter of which form Si₄ tetrahedra. BaSi₂ can be considered as Zintl phase.^{10,11} Revealing the valence band (VB) structure is indispensable to understand the optical and electronic properties of BaSi₂, which are responsible for the solar cell applications. Although several theoretical studies have discussed the density of states (DOS) of BaSi₂,^{3,12–14} the VB structure has yet to be examined experimentally. Photoelectron spectroscopy is a powerful tool as a direct probe of VB DOSs.¹⁵ In general, conventional photoelectron spectroscopy in the electron kinetic-energy range of 50–100 eV is quite surface sensitive due to the short electron inelastic mean free path (IMFP) of <5 Å. The electronic states at surface are strongly reflected in the photoelectron spectra, which makes it difficult to examine the electronic states inside the film. Although the larger probing depth than 50 Å could be expected with hard x-ray photons, a significantly reduced photoionization cross section prevented us from measuring valence-band photoelectron spectra above 3 keV.^{16,17} An extremely brilliant X-ray provided from the third generation synchrotron source can well compensate for

the diminished cross section and has enabled us to perform hard x-ray photoelectron spectroscopy (HAXPES) measurements with high-energy resolution.¹⁸ In this paper, we grew BaSi₂ epitaxial films on Si(111) substrates by molecular beam epitaxy (MBE) and evaluated its VB electronic structure near the Fermi level, E_F , using HAXPES.

II. EXPERIMENTAL METHOD

A CaF₂ (2 nm)/undoped BaSi₂ (35 nm) layered structure was grown epitaxially by MBE on *p*-type Si(111) substrates ($p = 1 \times 10^{19} \text{ cm}^{-3}$). A two-step growth method was adopted that included reactive deposition epitaxy (RDE; Ba deposition on hot Si) for BaSi₂ template layers, and subsequent MBE (MBE; codeposition of Ba and Si on Si) to form BaSi₂ overlayers.^{19,20} RDE growth was employed to form a template layer prior to the subsequent MBE process. Briefly, for RDE growth, we set the Ba deposition rate (R_{Ba}), the substrate temperature and the growth time as 1.0 nm/min, 510 °C, and 5 min, respectively. Then both Ba and Si were deposited on the template layers to form a 35-nm-thick BaSi₂ epitaxial layer by MBE at 580 °C for 30 min. The Si deposition rate was set at 1.0 nm/min for $R_{\text{Ba}} = 3.0 \text{ nm/min}$. The deposition rates of Si and Ba were monitored and controlled by a quartz crystal microbalance technique (IC/5, INFICON). After the growth of the BaSi₂ layer, an approximately 2-nm-thick CaF₂ capping layer was formed in the same MBE chamber at room temperature, in order to prevent oxidation of the BaSi₂ layer. We also calculated the DOSs of BaSi₂ using the CASTEP code based on the density-functional theory in description of the electron-electron interaction, a pseudopotential description of the electron-core interaction, and a plane-wave expansion of the wavefunction.^{12,13} The crystalline quality of the film was evaluated using reflection

high-energy electron diffraction (RHEED) and $\theta - 2\theta$ X-ray diffraction (XRD) measurements. HAXPES measurements were performed in a near normal emission geometry at the undulator beamline BL15XU (Ref. 18) of SPring-8 in Japan. We set the take-off angle θ and the incident light angle ($\theta - 90$) to 1 and 89° , respectively, with respect to the surface normal. This is not a surface-sensitive but a bulk-sensitive geometry. The excitation photon energy and overall energy resolution were set to 5953 eV and 150 meV, respectively. The position of E_F was determined with an evaporated Au film.

III. RESULTS AND DISCUSSION

Figures 1(a) and 1(b) exhibit RHEED patterns observed along Si[11-2] azimuth after the growth of BaSi₂ and CaF₂ layers, respectively. Sharp streaky patterns of BaSi₂ seen in Fig. 1(a) indicate that BaSi₂ with a flat surface was grown epitaxially. Moreover, the BaSi₂ surface was covered with amorphous-like CaF₂ as evidenced in Fig. 1(b). Figure 1(c) shows the $\theta - 2\theta$ XRD pattern of sample. We can see diffraction peaks only from (100)-oriented BaSi₂ planes, such as the (200), (400), and (600) planes. These results present that the highly *a*-axis-oriented BaSi₂ epitaxial film was grown.

The wide range HAXPES spectrum is shown in Fig. 2. We can see intense peaks corresponding to Ba, Si, Ca, and F atoms. On the other hand, the O 1s peak at -531 eV is negligibly small. Figure 3(a) shows the calculated partial DOSs of Si 3s, 3p, and Ba 6s, 6p and 5d states. The VBs consist of three parts in BaSi₂.^{3,12} Those shown in Fig. 3(a) correspond to the two of them located at energies closer to E_F . The Si 3s state appears dominant in the VB at around -6 eV, while the Si 3p state contributes significant to the VB extending from -4 eV to E_F . The bottom of the conduction band (CB) consists of a mixture of Si and Ba states. The fact that the experimentally obtained absorption coefficients are large in BaSi₂ (Ref. 2) is thus explained by the states across the gap which

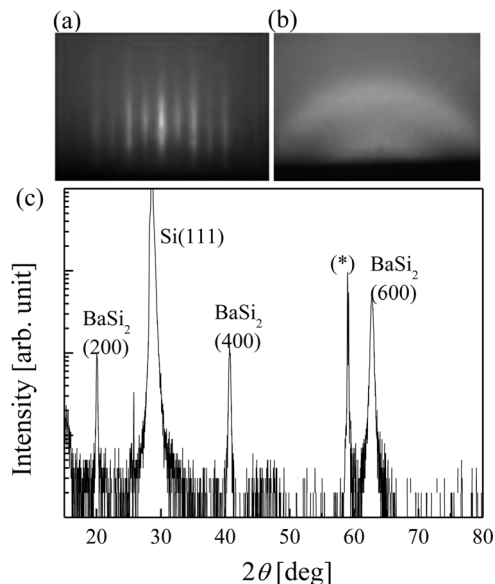


FIG. 1. RHEED patterns after the growth of (a) BaSi₂ and (b) CaF₂ layers observed along Si(11-2), and (c) θ - 2θ XRD pattern.

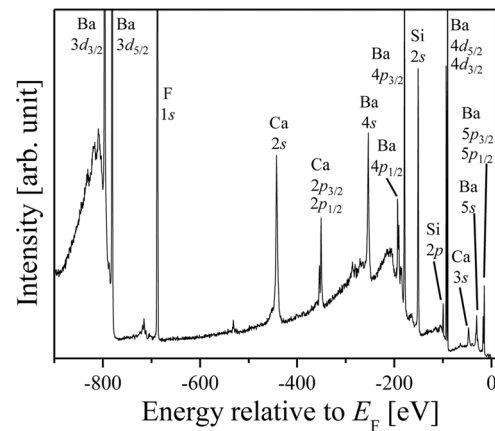


FIG. 2. Wide range HAXPES spectrum of sample.

are composed of a mixture of Si-*sp* and Ba-*pd* states, leading to large values of dipole matrix elements. Before comparing the theoretical DOS with the VB HAXPES spectrum, the partial DOSs of BaSi₂ in Fig. 3(a) are rescaled by considering the photo-ionization cross-sections at a photon energy of 6 keV as shown in Fig. 3(b). The cross sections for Si 3s and 3p and Ba 6s states at this energy are estimated to be

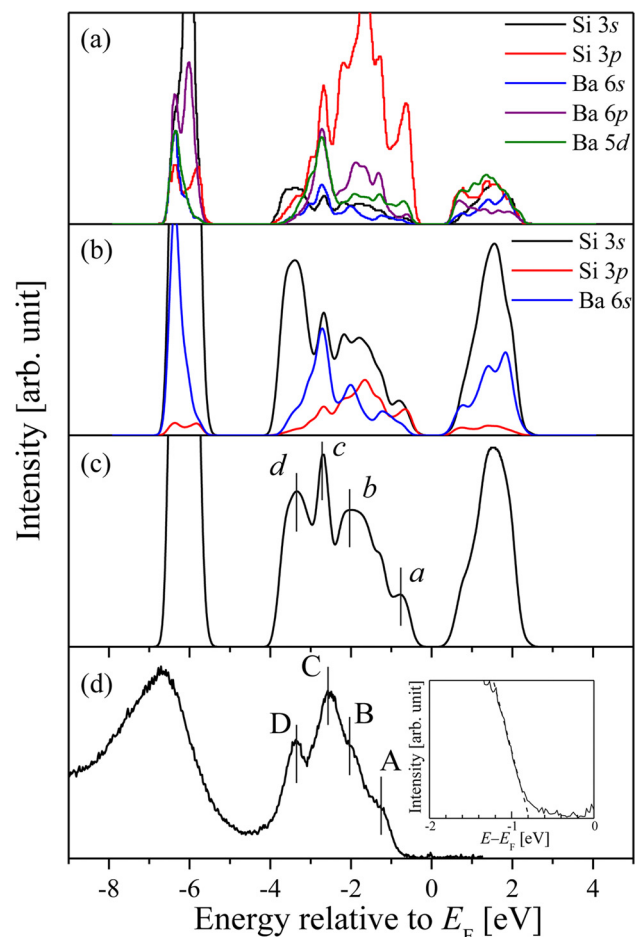


FIG. 3. (a) Partial DOSs of Si 3s, 3p, Ba 6s, 6p, and 5d states, (b) calculated photoemission spectra of Si 3s, Si 3p and Ba 6s states using the partial DOSs of BaSi₂ multiplied by the photo-ionization cross-sections at 6 keV. (c) Expected photoelectron spectrum. (d) HAXPES spectrum for BaSi₂ measured at a photon energy of 5953 eV.

1.69×10^{-23} , 8.13×10^{-25} , and $1.04 \times 10^{-23} \text{ cm}^2$, respectively.^{16,17} The ratio of Si(3s)/Si(3p) is 20.8, and that of Si(3s)/Ba(6s) is 1.63. It thus means that the Si 3s state contributes to the HAXPES spectrum significantly although the Si 3p state dominates in the original VB DOS near E_F in Fig. 3(a). Figure 3(c) shows the expected spectrum, which is the sum of the rescaled partial DOSs of Si 3s, Si 3p, and Ba 6s states shown in Fig. 3(b). Figure 3(d) shows the experimentally obtained HAXPES spectrum. We are not able to estimate the contributions of Ba 6p and 5d states in the expected spectrum in Figs. 3(b) and 3(c) although they actually contribute to the VB DOSs as shown in Fig 3(a). This is because their photo-ionization cross-sections at the photon energy of 6 keV are not available due to their unoccupied orbitals in individual atoms. The HAXPES spectrum in Fig. 3(d) can be reasonably explained by the spectrum in Fig. 3(c). The structures labeled A-D in Fig. 3(d) match well with those labeled a-d in Fig. 3(c). Structures A and B are explained by the Si 3s, Si 3p, and Ba 6s states. The Ba 6s state contributes to structure C. Structure D is explained by the Si 3s state. The inset in Fig. 3(d) shows the spectrum near -1.0 eV , indicating that the VB top, E_V , is located about 0.8 eV below E_F . Since the size of the band gap of BaSi₂ is about 1.3 eV ,² the spectrum is shifted downwards a little probably due to n -type conductivity of the grown BaSi₂ film.¹ The separation of the bottom of the conduction band, E_C , from E_F , that is $E_C - E_F$, is thus estimated to be about 0.5 eV . Assuming that the effective density of states of CB, N_C , is approximately $2.6 \times 10^{19} \text{ cm}^{-3}$,²¹ the value of electron concentration, n , is derived to be about $1 \times 10^{11} \text{ cm}^{-3}$ using

$$n = N_C \exp\left(-\frac{E_C - E_F}{k_B T}\right), \quad (1)$$

where k_B is the Boltzmann constant, and T the absolute temperature. This value is much smaller than $n = 5 \times 10^{15} \text{ cm}^{-3}$,¹ which is usually obtained for undoped BaSi₂ films on high-resistive n -type Si(111) substrates ($n \sim 10^{12} \text{ cm}^{-3}$). This small electron density ($n = 1 \times 10^{11} \text{ cm}^{-3}$) is probably caused by the depletion of the BaSi₂ film (35 nm) because of the heavily p -type Si substrate ($p = 1 \times 10^{19} \text{ cm}^{-3}$) used in this work.

Figure 4 shows the calculated band profile of a 35-nm-thick undoped BaSi₂ ($n = 5 \times 10^{15} \text{ cm}^{-3}$)/ p -Si(111) ($p = 1 \times 10^{19} \text{ cm}^{-3}$) together with a 2-nm-thick thin CaF₂ capping layer. Due to the difference in electron affinity between Si, BaSi₂, and CaF₂, and the large band gap of CaF₂ (12.1 eV),²² there are band offsets at the heterointerface. In the calculation, we used the electron affinities of Si, BaSi₂, and CaF₂ to be 4.0, 3.3, and 1.8 eV, respectively.^{23–25} As shown in Fig. 4, the VB of CaF₂ is located far below that of BaSi₂ due to the large band gap of CaF₂. For this reason, it is reasonable to think that the contribution of the 2-nm-thick CaF₂ to the measured VB spectrum, shown in Fig. 3(d) can be neglected especially for the VB spectrum around the top of VB. We see that the band bending occurs in the BaSi₂ as shown in Fig. 4, meaning that there is the electric field within the BaSi₂ layer. The electric field could affect the line shape of the XPS spectrum and cause the shift of peak position.²⁶

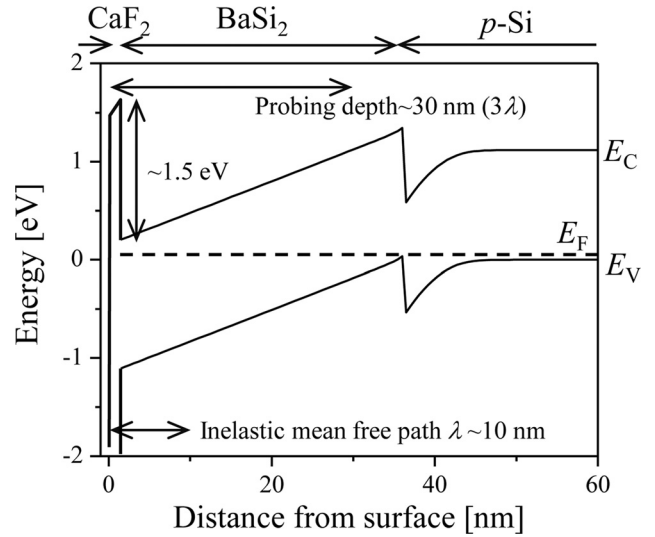


FIG. 4. Band profile near the interface of undoped n -BaSi₂ ($n = 5 \times 10^{15} \text{ cm}^{-3}$)/ p -Si(111) ($p = 1 \times 10^{19} \text{ cm}^{-3}$). The E_V is set at $E = 0 \text{ eV}$.

Regarding core level excitations such as Ba 3d, 4s and 4p states shown in Fig. 2, these peaks are sharp, and their peak shifts are as small as the measurement energy resolution. Thus, we think that the influence of the electric field on the HAXPES spectrum is considered small. The IMFP value, λ , is calculated to be approximately 10 nm for BaSi₂ at 6 keV from the Tanuma-Powell-Penn equation.²⁷ Assuming that the HAXPES signal intensity decays as $\exp(-x/\lambda)$ at a depth x beneath the surface, the probability of escape of the photoelectron in a direction normal to the surface and without inelastic scattering is $\exp(-3) \sim 5\%$ when $x = 3\lambda$. This means that virtually all of the electrons ($\sim 95\%$) detected come from the surface within 3λ . The probing depth is thus estimated to be approximately $3\lambda \times \cos(\theta) \sim 30 \text{ nm}$ when $\theta = 1^\circ$. Assuming that the XPS signal intensity varies as $\exp(-x/\lambda)$, the separation of E_F from E_V , that is $\langle E_F - E_V \rangle$, is expected to be about 0.75 eV from

$$\langle E_F - E_V \rangle \approx \frac{\int_0^{3\lambda} (E_F - E_V) \exp(-x/\lambda) dx}{\int_0^{3\lambda} \exp(-x/\lambda) dx}, \quad (2)$$

where t is the CaF₂ layer thickness. This value agrees well with the experimental result shown in the inset of Fig. 3(d). This means that the measured value of $E_V - E_F$ shown in the inset of Fig. 3(d) is consistent with the band structure in Fig. 4.

On the basis of the results presented, we confirmed that the Si 3s and 3p states contribute mostly to the top of VB in BaSi₂ as expected from theory. This is the same as in Si. Undoped n -type BaSi₂ has a long minority-carrier diffusion length of approximately $10 \mu\text{m}$,⁶ and thus can be utilized as a light absorbing layer in a solar cell. The effective mass of holes is critical because the photogenerated minority carriers are holes in n -type BaSi₂, and they play an important role in

the transport of photogenerated carriers. The approximate average effective mass of holes was calculated to be $0.53m_0$ from the principal-axis components of the effective-mass tensor for holes reported in Ref. 3. Here, m_0 is the free electron mass. This value is relatively small and comparable to that of Si,²³ meaning that undoped *n*-type BaSi₂ is considered promising as a light absorbing layer in solar cells.

IV. SUMMARY

CaF₂ (2 nm)/BaSi₂ (35 nm)/Si(111) was grown by MBE, and the VB structure of BaSi₂ was characterized by hard HAXPES. Structures observed in the HAXPES spectrum were well explained by the calculated photoemission spectra of Si 3*s*, Si 3*p*, and Ba 6*s* states. The observed spectrum was shifted a little to a lower energy due to *n*-type conductivity of the BaSi₂, and the band bending in the BaSi₂. The fact that the top of the VB consists mainly of Si 3*s* and 3*p* states in BaSi₂ is favorable in solar cell applications. This is because small effective mass of holes is available when we use this undoped low-*n* BaSi₂ layer as a light absorption layer for photogenerated holes.

ACKNOWLEDGMENTS

The HAXPES measurements were performed at Synchrotron X-ray Station of BL15XU, at SPring-8, NIMS (Proposal No. 2012B4908). This work was financially supported by the Japan Science and Technology Agency (JST/CREST).

¹K. Morita, Y. Inomata, and T. Suemasu, *Thin Solid Films* **508**, 363 (2006).

²K. Toh, T. Saito, and T. Suemasu, *Jpn. J. Appl. Phys.* **50**, 068001 (2011).

³D. B. Migas, V. L. Shaposhnikov, and V. E. Borisenko, *Phys. Status Solidi B* **244**, 2611 (2007).

⁴W. Du, M. Suzuno, M. Ajmal Khan, K. Toh, N. Nakamura, M. Baba, K. Toko, N. Usami, and T. Suemasu, *Appl. Phys. Lett.* **100**, 152114 (2012).

⁵K. O. Hara, N. Usami, K. Toh, M. Baba, K. Toko, and T. Suemasu, *J. Appl. Phys.* **112**, 083108 (2012).

⁶M. Baba, K. Toh, K. Toko, N. Saito, N. Yoshizawa, K. Jiptner, T. Sekiguchi, K. Hara, N. Usami, and T. Suemasu, *J. Cryst. Growth* **348**, 75 (2012).

⁷M. Kobayashi, Y. Matsumoto, Y. Ichikawa, D. Tsukada, and T. Suemasu, *Appl. Phys. Express* **1**, 051403 (2008).

⁸M. Ajmal Khan, K. O. Hara, W. Du, M. Baba, K. Nakamura, M. Suzuno, K. Toko, N. Usami, and T. Suemasu, *Appl. Phys. Lett.* **102**, 112107 (2013).

⁹K. Nakamura, M. Baba, M. Ajmal Khan, W. Du, M. Sasase, K. O. Hara, U. Usami, K. Toko, and T. Suemasu, *J. Appl. Phys.* **113**, 053511 (2013).

¹⁰J. Evers, G. Oehlinger, and A. Weiss, *Angew. Chem., Int. Ed.* **16**, 659 (1977).

¹¹M. Imai and T. Hirano, *J. Alloys Compd.* **224**, 111 (1995).

¹²Y. Imai and A. Watanabe, *Intermetallics* **10**, 333 (2002).

¹³Y. Imai, A. Watanabe, and M. Mukaida, *J. Alloys Compd.* **358**, 257 (2003).

¹⁴S. Kishino, T. Imai, T. Iida, Y. Nakaishi, M. Shinada, Y. Takanashi, and N. Hamada, *J. Alloys Compd.* **428**, 22 (2007).

¹⁵M. Sumiya, M. Lozach, N. Matsuki, S. Ito, N. Ohhashi, K. Sakoda, H. Yoshikawa, S. Ueda, and K. Kobayashi, *Phys. Status Solidi C* **7**, 1903 (2010).

¹⁶M. B. Trzhaskovskaya, V. I. Nefedov, and V. G. Yarzhemsky, *At. Data Nucl. Data Tables* **77**, 97 (2001).

¹⁷M. B. Trzhaskovskaya, V. I. Nefedov, and V. G. Yarzhemsky, *At. Data Nucl. Data Tables* **82**, 257 (2002).

¹⁸S. Ueda, Y. Katsuya, M. Tanaka, H. Yoshikawa, Y. Yamashita, S. Ishimaru, Y. Matsushita, and K. Kobayashi, *AIP Conf. Proc.* **1234**, 403 (2010).

¹⁹Y. Inomata, T. Nakamura, T. Suemasu, and F. Hasegawa, *Jpn. J. Appl. Phys., Part 1* **43**, 4155 (2004).

²⁰Y. Inomata, T. Nakamura, T. Suemasu, and F. Hasegawa, *Jpn. J. Appl. Phys., Part 2* **43**, L478 (2004).

²¹D. B. Migas, private communication (2013).

²²G. W. Rubloff, *Phys. Rev. B* **5**, 662 (1972).

²³S. M. Sze, *Physics of Semiconductor Devices*, 2nd ed. (Wiley, New York, 1981), p. 850.

²⁴T. Suemasu, K. Morita, M. Kobayashi, M. Saida, and M. Sasaki, *Jpn. J. Appl. Phys., Part 2* **45**, L519 (2006).

²⁵A. Izumi, Y. Hirai, K. Tsutsui, and N. S. Sokolov, *Appl. Phys. Lett.* **67**, 2792 (1995).

²⁶H. Kobayashi, K. Namba, Y. Yamashita, Y. Nakato, and Y. Nishioka, *Surf. Sci.* **357–358**, 455 (1996).

²⁷S. Tanuma, C. J. Powell, and D. R. Penn, *Surf. Interface Anal.* **43**, 689 (2011).